Journal of Fluid Science and Technology

Vol. 7, No. 3, 2012

Temperature Characteristics of Backlayering Thermal Fumes in a Tunnel Fire*

Katsushi FUJITA**, Tomoya MINEHIRO***, Nobuyoshi KAWABATA**** and Futoshi TANAKA*****

**Department of Mechanical Engineering, Fukui National College of Technology, Geshi-cho, Sabae-shi, Fukui 916-8507, JAPAN
E-mail: fujita@fukui-nct.ac.jp

***Graduate School of Natural Science and Technology, Kanazawa University, Kakuma-machi, Kanazawa-shi, Ishikawa 920-1192, JAPAN
E-mail: minehiro@stu.kanazawa-u.ac.jp

****School of Mechanical Engineering, Kanazawa University, Kakuma-machi, Kanazawa-shi, Ishikawa 920-1192, JAPAN
E-mail: kwbt@t.kanazawa-u.ac.jp

*****Department of Mechanical Engineering, University of Fukui, 3-9-1 Bunkyo, Fukui-shi, Fukui 910-8507, JAPAN
E-mail: f-tanaka@u-fukui.ac.jp

Abstract

In this study, we used a 1/5-scale model tunnel to investigate the temperature characteristics of backlayering thermal fumes in addition to the heat release rate and the longitudinal ventilation velocity in a tunnel fire. The ventilation flow through the model tunnel provided a sufficient turbulent flow as the Reynolds number based on ventilation velocity and tunnel height was 40,000 or more. The governing scaling parameter in this experiment was the dimensionless parameter Q^*/Fr. In addition to Froude's and Reynolds' similarity laws, the similarity of the thermal characteristics in the tunnel wall was considered in making the model tunnel. We clarify the conditions under which the backlayering thermal fumes maintain a stratified layer. Empirical equations of the thermal fume height in the longitudinal ventilation are derived from the experimental data. The evacuation safety based on the height of thermal fumes is examined in detail.

Key words: Tunnel Fire, Backlayering Thermal Fumes, Temperature Distribution, Turbulent Flow, Stratified Flow, Model Experiment, Flow Measurements

1. Introduction

In a normal enclosed tunnel, the length is larger than the cross section. In the event of a tunnel fire, thermal fumes generated by the fire quickly fill the tunnel due to its limited width. Moreover, securing the evacuation environment and performing fire fighting and rescue operations are hampered by reduced visibility from smoke. As a result, serious fire damage and injuries frequently occur[(1)(2)]. In order to effectively reduce the risk of damage and injuries in a tunnel fire, it is necessary to clarify the fire properties, such as the behavior of thermal fumes generated by a fire.

Japan's expressway tunnels, which are generally unidirectional, adopt a longitudinal ventilation system that blows parallel to the direction of passing vehicles. In the event of a fire, emergency longitudinal ventilation measures in a one-way tunnel are as follows. Thermal fumes are swept away in the downstream direction from the fire source by the

*Received 29 Jan., 2012 (No. T2-09-1056)
Japanese Original : Trans. Jpn. Soc. Mech. Eng., Vol.76, No.768, B (2010), pp.1176-1183 (Received 30 Nov., 2009)
[DOI: 10.1299/jfst.7.275]

ventilation wind. Upstream, where the traffic jam is, backlayering of thermal fumes is prevented by the ventilation wind, allowing safe evacuation from the vehicles. The velocity of ventilation wind required to prevent the spread of backlayering thermal fumes is called the critical velocity, and it is extensively studied using analytical theories[3][4], fire experiments[5]-[11], and numerical simulation[12]. On the other hand, the backlayering distance and temperature distribution of thermal fumes are also important characteristics of a tunnel fire. Studies have been conducted based on model experiments[11][13][14] and numerical simulation[15][16], but sufficient engineering knowledge has not yet been obtained. Consequently, we developed a large-scale model tunnel and carried out numerous fire experiments.

The purpose of the present study was to grasp the flow characteristics of backlayering thermal fumes in a tunnel fire when longitudinal ventilation wind is blowing through the tunnel. The large-scale model tunnel used for the fire experiments was compared to the models used in previous studies in consideration of Reynolds' scaling law[5][8][10][11]. The temperature distribution, velocity of longitudinal ventilation, and heat release rate of the fire source were measured under the conditions of four different sized fires. Particularly, temperature distribution was simultaneously measured at a number of points at the ceiling and longitudinal section of the model tunnel. The results of detailed temperature distribution more than those obtained in previous studies were obtained in this research. Based on those results, the temperature distribution of the thermal fumes generated by the tunnel fire was examined. We report on new engineering knowledge concerning the evacuation environment under thermal fumes and the temperature distribution of the backlayering thermal fumes.

2. Nomenclature

A : Cross-section of tunnel [m^2]
A_f : Burning area [m^2]
Bi : Biot number [-] $Bi = hH/\lambda$
Fo : Fourier number [-] $Fo = \alpha\sqrt{H/g}\,/H^2$
Fr : Froude number $Fr = U_{ms}/\sqrt{gH}$ [-]
g : Gravitational acceleration [m/s^2]
H : Height of tunnel (characteristic length) [m]
H_{dT} : Height of boundary between thermal fumes and fresh air [m]
H^*_{dT} : Dimensionless height of boundary of thermal fumes $H^*_{dT} = H_{dT}/H$ [-]
h : Heat-transfer coefficient [W/m^2K]
L_b : Backlayering distance of thermal fumes [m]
Q : Heat release rate [W]
Q_m : Average quasi-steady heat release rate [W]
Q_{max} : Quasi-steady heat release rate [W]
Q^* : Dimensionless quasi-steady heat release rate $Q^* = Q_{max}/(\rho_0 C_p T_0 A\sqrt{gH})$ [-]
Q^*_m : Average dimensionless quasi-steady heat release rate [-]
Re : Reynolds number $Re = U_{ms}H/\nu$ [-]
T_0 : Ambient temperature [K]
U_m : Velocity of longitudinal ventilation [m/s]
U_{ms} : Average velocity of longitudinal ventilation (characteristic velocity) [m/s]
x^* : Dimensionless coordinate in tunnel length $x^* = x/H$ [-]
y^* : Dimensionless coordinate in tunnel width $y^* = y/H$ [-]

z^* : Dimensionless coordinate in tunnel height $z^* = z/H$ [-]
α : Thermal diffusivity [m^2/s]
δT : Temperature rise [K]
δT^* : Dimensionless temperature rise $\delta T^* = \delta T/T_0$ [-]
λ : Thermal conductivity [W/mK]
γ : Scale ratio [-]
ν : Kinematic viscosity [m^2/s]
ρ_0 : Air density at ambient temperature [kg/m^3]

3. Experimental facility and instruments

3.1 Model tunnel

The model tunnel in this study was scaled to 1/5 the size of a full-scale tunnel. Various parameters were decided based on the respective scaling laws[17]. Table 1 shows the parameters of both the model tunnel and a full-scale tunnel, and the parameters of model tunnels of other researchers. The longitudinal ventilation velocity U_m and heat release rate Q of a full-scale tunnel were calculated by using the Froude scaling law based on the parameters of our model tunnel.

In this study, the governing scaling parameter in a tunnel fire with longitudinal ventilation is the dimensionless parameter Q^*/Fr. The Froude number Fr is defined as the ratio of the buoyancy of a plume generated by a fire source and the inertia force of the longitudinal ventilation wind. The dimensionless heat release rate Q^* is defined as the ratio of the heat release rate and the enthalpy flow rate. The enthalpy flow rate when air at the temperature T_0 flows in a tunnel with cross-section A at velocity $\sqrt{gH}$ is used as the characteristic parameter of the heat release rate. The ratio of the characteristic length L_f of a full-scale tunnel and the characteristic length L_m of the model tunnel is defined as the scale ratio $\gamma = L_f/L_m$. It was found that the longitudinal ventilation velocity U_m is proportional to $\gamma^{0.5}$, and the heat release rate Q is proportional to $\gamma^{2.5}$ by using Froude scaling.

It was important to achieve a completely turbulent flow in the model tunnel as well as a full-scale tunnel for the model experiment. The model tunnel in this study is at least three times as large as the model tunnels of other researchers, as shown in Table 1. Therefore, the Reynolds number Re of the ventilation flow in the model tunnel is 40,000 or more, and a completely turbulent flow is achieved in the tunnel. On the other hand, the Reynolds number Re in the other studies ranges from a few thousand to 30,000; part of the flow through a tunnel in such a small Reynolds number may not be a turbulent flow.

The heat transfer phenomenon from the thermal fumes to the wall of the tunnel is an important governing phenomenon in a tunnel fire. The amount of heat transfer is governed by the conduction heat transfer characteristics of the materials inside the wall and the convection heat transfer characteristics on the surface of the wall. Table 1 indicates the Biot number Bi and the Fourier number Fo concerning thermal characteristics of the wall of each tunnel. Contrary to the other studies, these values for the model tunnel in the present study are close to the values of a full-scale tunnel made of concrete. Autoclaved lightweight aerated concrete (ALC) panel was used as a suitable wall material for the model tunnel in the present study. In the other studies, the value of the Fourier number in the model tunnel is especially large compared with that of a full-scale tunnel. In these cases, the wall of the model tunnel has a large thermal conductivity in contrast to the wall of a full-scale tunnel made of concrete. Therefore, it is considered that there is too much absorption of heat flux from the thermal fumes.

Figure 1 shows a schematic diagram of the experimental apparatus, which comprises the

model tunnel part and the chamber part. The thermal fumes that flow out from the model tunnel part are discharged outside by blowers in the chamber part. A stainless-steel combustion vessel was installed as the fire source in the center, 32.1 m from the tunnel opening. n-Heptane (lower heating value: 44.56 MJ/kg), which is a main constituent of gasoline, was used as the fuel for the fire source. The origin of the coordinates is the position of the fire source. The size of the model tunnel part is as follows: 41.4 m in total length (x-coordinate), 1.93 m in width (y-coordinate), and 1 m in height (z-coordinate). The cross section of the model tunnel is rectangular.

Table 1 Properties of the model tunnel, a full-scale tunnel and the tunnels of other studies

	Present	-	Lee[8]	Roh[10]	Oka[5]	Yamada[11]
Type	Model tunnel	Full-scale tunnel	Model tunnel	Model tunnel	Model tunnel	Model tunnel
Section	Rectangular	Rectangular	Rectangular	Horseshoe	Horseshoe	Square
Height H [m]	1	5	0.3–0.6	0.4	0.244	0.3
Width B [m]	1.93	10	0.6–0.3	0.4	0.274	0.3
U_{ms} [m/s]	0.61–1.67	1.36–3.73	0.40–0.57	0.44–1.68	0.12–0.52	0.20–0.67
Re	41000–110000	450000–1200000	8100–26000	18000–27000	1900–8200	3900–13000
Fr	0.19–0.53	0.19–0.53	0.19–0.34	0.22–0.85	0.078–0.34	0.12–0.40
Q [MW]	0.066–0.377	3.63–21.8	0.0025–0.012	0.0044–0.017	0.00035–0.03	0.002–0.008
Q^*	0.032–0.182	0.032–0.182	0.019–0.11	0.054–0.14	0.0034–0.3	0.037–0.146
Material (Near fire)	ALC	Concrete	Acrylic resin (Gypsum board)	Acrylic resin (Steel)	Perspex (steel)	Ceramic fiberboard
Bi	41.2–117.6	21.9–65.5	19–55	19–55	8.54–22.4	7.9–64
Fo	6.41×10^{-8}	2.37×10^{-8}	1.2×10^{-7}	1.2×10^{-7}	3.1×10^{-7}	2.5×10^{-6}–8.7×10^{-7}

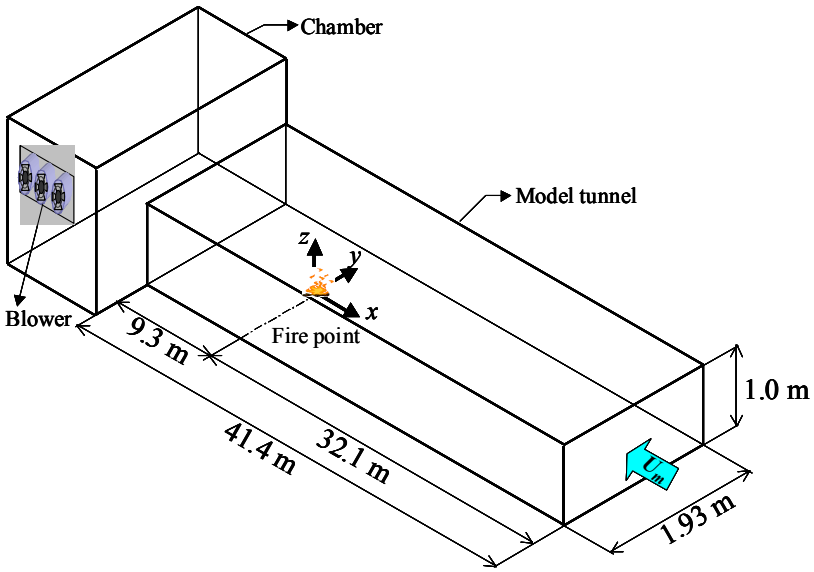

Fig. 1 Schematic diagram of the experimental apparatus

3.2 Measurement items

3.2.1 Heat release rate

There are two main methods for measuring the heat release rate Q. One is a direct method that calculates the heat release rate from the burning rate of fuel measured by an electric balance[17]. The other is an indirect method that calculates the heat release rate from the amount of radiant heat flux of fire measured by a radiometer[18]. The direct method was mainly used to measure the heat release rate in the present study. An electric balance C

(Mettler Toledo SB16000) was installed outside the tunnel, as shown in Fig. 2(a). A combustion vessel A was placed on the support stand of the electric balance. The burning rate of fuel in the vessel was measured by using the electric balance at 1-s intervals. The heat release rate was calculated by multiplying the burning rate by the lower heating value of the fuel.

Radiometer B (Tokyo Seiko Co., Ltd. Type RE-4) was installed upstream from the fire; the installation coordinates were x = 1.5 m, y = 0 m, and z = 0.2 m, respectively. Radiant heat flux from the fire was acquired at 0.2-s intervals. The radiant heat from a fire is generally proportional to the burning rate of the fire in a tunnel with longitudinal wind[18]. It is assumed that the time curves of the radiant heat from the fire and the heat release rate of the fire are similar. The proportionality coefficient between the time integration value of the radiant heat measured with the radiometer and the total calorific value of fuel was calculated. The time curve of the heat release rate was computed by multiplying the measurement value of the radiant heat by this coefficient.

3.2.2 Longitudinal wind velocity

The velocity of longitudinal ventilation U_m through the model tunnel was measured by anemometers (Kanomax Climomaster Model 6543) installed in four locations upstream from the fire: x = 24.5 m, (y, z) = (0.5, 0.25 m), (0.5, 0.85 m), (−0.5, 0.25 m), (−0.5, 0.85 m). The wind velocity was acquired at 1.0-s intervals.

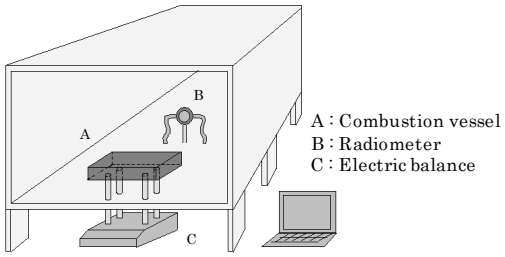

(a) Installation conditions of electric balance and radiometer

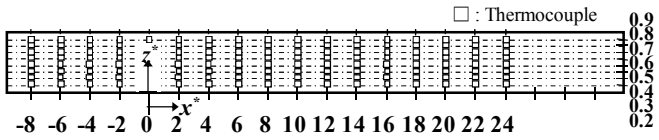

(b) Placement of thermocouples in central longitudinal section (y^* = 0.0)

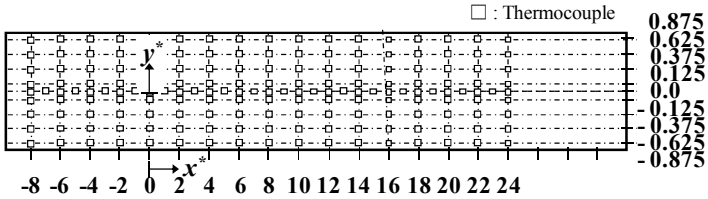

(c) Placement of thermocouples under the ceiling (z^* = 0.98)

Fig. 2 Schematic diagram of measurement systems for heat release rate and temperature

3.2.3 Temperature

The temperature inside the model tunnel was measured by thermocouples placed at a total of 297 points on the ceiling and central longitudinal section of the model tunnel. The K-type thermocouple of 0.1 mm in diameter with a small time constant was used for temperature measurement. Thermocouples at 8 locations in the direction of the tunnel height were installed at 2-m intervals in the central longitudinal section, as shown in Fig. 2(b). Thermocouples at 128 locations were installed in the central longitudinal section. The thermocouples at 9 locations in the direction of the tunnel width were installed at 2-m intervals under the ceiling, as shown in Fig. 2(c). These thermocouples were installed 20 mm directly below the ceiling. In addition, thermocouples under the ceiling were installed in the central line (y = 0 m) at 1-m intervals. Thermocouples at 169 locations were installed under the ceiling. The temperature was acquired by a data logger (Keyence NR250) at 1.0-s intervals.

3.3 Experimental conditions

The velocity of the longitudinal wind was examined in the range of 0.61 to 1.67 m/s, which corresponds to 1.36 to 3.73 m/s of the ventilation velocity of a full-scale tunnel (scale ratio γ = 5). Fire scales were 65, 170, 240, and 390 kW (burning area of combustion vessel: 0.079, 0.15, 0.18, 0.22 m^2), respectively. These heat release rates are equivalent to a fire scale of 3.63, 9.50, 13.4, and 21.8 MW in a full-scale tunnel (scale ratio γ = 5). In the case of 3.63 and 21.8 MW, this is equivalent to one passenger vehicle and one bus on fire, respectively, as suggested by the PIARC Committee[(2)].

4. Quasi-steady condition

Figures 3 and 4 show the measurement results in the cases of a burning area of A_f = 0.15 and 0.079 m^2, respectively. The time curves of the rise in temperature at several measurement positions are shown in the upper parts of the figures. The time curves of the heat release rate and velocity of longitudinal ventilation are shown in the lower parts of the figures. Each of the time curves of the heat release rate measured by using the electric balance (direct method) and the radiometer (indirect method) is shown in the lower parts of these figures. The average value for 15 s of the heat release rate is also shown. The results with the electric balance and the radiometer are indicated by inverse triangles and diamonds, respectively. The heat release rate increases rapidly with ignition (t = 0 s), and then gradually approaches a steady condition. The time curves of the heat release rate measured by the direct and the indirect methods are in agreement. Since the time constant of the radiometer used in this experiment is a large value, the method using the radiometer has a time lag compared with the method with the electric balance, but the differences are insignificant. The heat release rate maintains a constant value for a short time in both time curves. In this study, the time range in which the fluctuation of the average value for 15 s of the heat release rate is less than 5% and the time range including the maximum heat release rate were defined as a quasi-steady condition. We focused on the quasi-steady condition as follows. Within the range of the experimental conditions of this study, the quasi-steady condition was maintained for one moment in all of the experimental cases. In addition, the range of the quasi-steady condition of the heat release rate measured with the electric balance and the radiometer was in agreement for 30 s or more in all of the experimental cases. In this study, the quasi-steady heat release rate Q_{max} was defined as the average value for 30 s of the quasi-steady condition including the maximum heat release rate.

The time curves of the longitudinal ventilation velocity and the temperature rise in the central section under the ceiling are shown in Figs. 3 and 4. The time curve of the average value measured by the anemometers at four positions is shown as the velocity of the

longitudinal ventilation U_m. The average velocity of the longitudinal ventilation U_{ms} in the same time range as the quasi-steady heat release rate Q_{max} was defined as the characteristic velocity. The difference between instantaneous velocity and the average velocity was defined as the fluctuation of wind velocity. The range of the fluctuation was 5% or less of the average velocity. The average value of the temperature rise in the same time range as the quasi-steady heat release rate was defined as the temperature rise in the quasi-steady condition. The difference between instantaneous temperature rise and the average value of temperature rise was defined as the fluctuation of temperature rise as in the case of the wind velocity. The range of the fluctuation of the temperature rise was 5% or less of the average temperature.

Figure 5 shows the relationship of the quasi-steady heat release rate Q_{max} measured by the electric balance and the average velocity of the longitudinal ventilation U_{ms}. The quasi-steady heat release rate Q_{max} tends to decrease slightly with the increase of the average longitudinal velocity U_{ms}. However, this slight change is disregarded in this study. The average quasi-steady heat release rate Q_m is calculated for each burning area of the combustion vessel using the data of Q_{max} in Fig. 5. Table 2 shows the average quasi-steady heat release rate Q_m for each burning area (A_f = 0.079, 0.15, 0.18, 0.22 m^2). The heat release rate of this experiment is larger than that of the other experiments, as shown in Table 1. Q_m of this experiment ranges from 66.2 to 377.4 kW, as shown in Table 2. As shown in Table 1, the value of Q_m in the study by Lee et al.[8] was in the range of 2.5 to 12 kW. In the study by Roh et al.[10] the range was 4.4 to 17 kW, for Oka et al.[5] it was 0.35 to 3 kW, and for Yamada at el.[11] 2 to 8 kW. The value of Q_m corresponding to the size of a full-scale tunnel (scale ratio γ = 5) is also shown in Table 2.

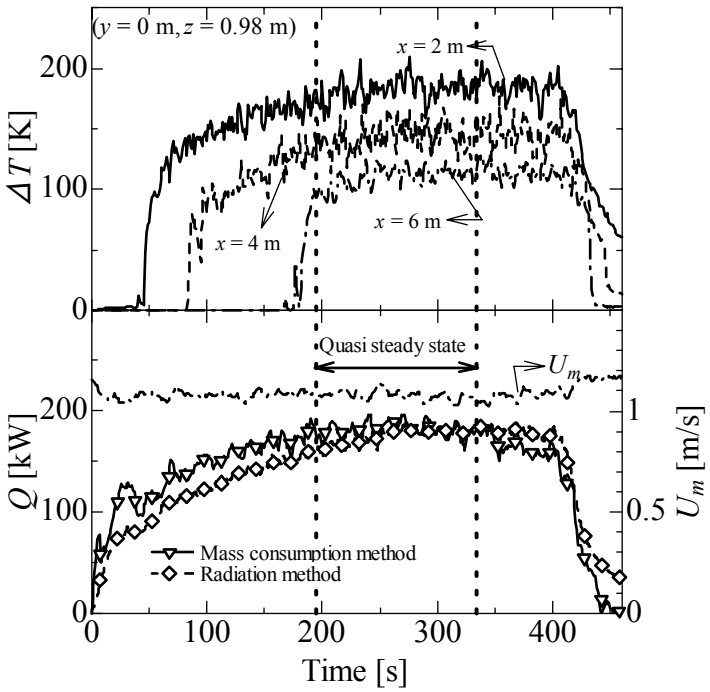

Fig. 3 Time curves of the heat release rate measured by an electric balance and a radiometer, ventilation velocity measured by anemometers installed in four positions, and temperature rise at thermocouples in three different positions: x = 2, 4, 6 m, y = 0 m, z = 0.98 m, in the case of the burning area A_f = 0.15 m^2

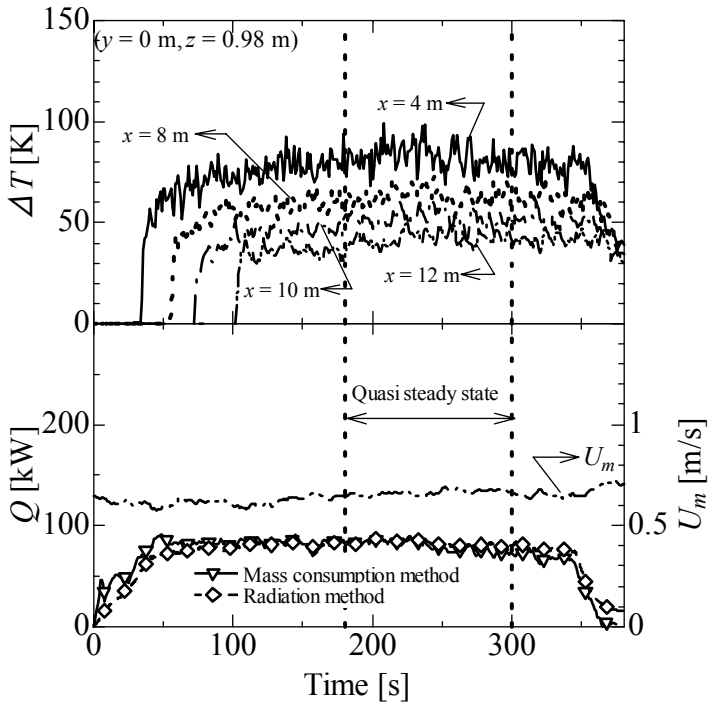

Fig. 4 Time curves of the heat release rate, ventilation velocity, and temperature rise at thermocouples in four different positions: x = 4, 8, 10, 12 m, y = 0 m, z = 0.98 m, in the case of the burning area A_f = 0.079 m^2

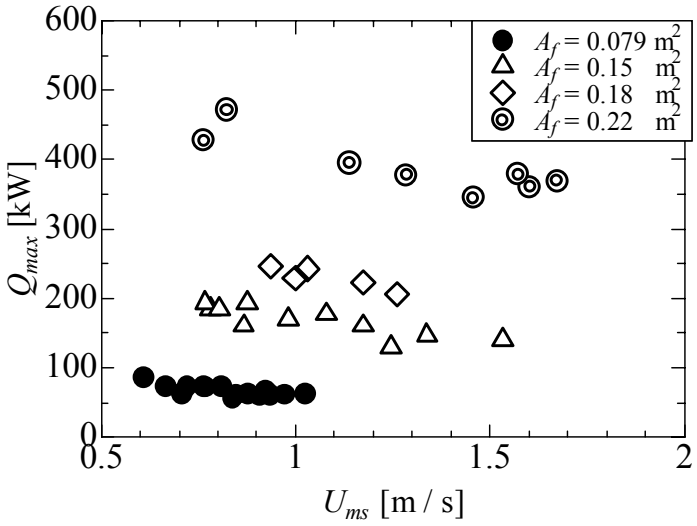

Fig. 5 Relationship between the quasi-steady heat release rate Q_{max} and the average velocity of the longitudinal ventilation U_{ms} in the four different burning areas A_f = 0.079, 0.15, 0.18, and 0.22 m^2

Table 2 Average heat release rate Q_m of each burning area A_f of the combustion vessel

Burning area A_f [m^2]	Electric balance Q_m [kW]	Radiometer Q_m [kW]	Q^*_m	Full-scale (Electric balance) [MW]
0.079	66.2	70.2	0.0316	3.70
0.15	165.3	173.5	0.0775	9.24
0.18	229.4	242.2	0.111	12.82
0.22	377.4	393.0	0.182	20.9

5. Temperature distribution of thermal fumes

The velocity of longitudinal ventilation during a fire in a one-way tunnel is 2 m/s in the Japanese standards, which corresponds to Froude number Fr = 0.29 in a full-scale tunnel having a height of 5 m.

Figure 6 shows the contour map of the temperature rise in the central longitudinal section and under the ceiling of the model tunnel under the conditions of the Froude number Fr in the range of 0.25 to 0.27 close to 0.29, and the average dimensionless quasi-steady heat release rate Q^*_m as a variable parameter. The temperature at the ceiling was measured by thermocouples installed 20 mm below the ceiling. The temperature distribution at the ceiling is shown by the contour line dividing the range of temperature from T^* = 0.034 (δT = 10K) to T^* = 1.01 (δT = 300K) into 30 levels. The temperature distribution in the central longitudinal section is shown by the contour line dividing the same range of temperature into 10 levels. A part of the contour line in the figure is not drawn on the map. The position of the fire source is x^* = 0. Thermocouples are not installed at this position. Under the conditions of each average dimensionless quasi-steady heat release rate Q^*_m, the thermal fumes maintain stratified layers in the upstream section from the fire source. The thermal fumes do not diffuse in the direction of the road. On the other hand, in the case of $Q^*_m \geq$ 0.182, the thermal fumes spread over the road of the tunnel in the section downstream from the fire source. When the average dimensionless quasi-steady heat release rate Q^*_m is in the range of less than 0.182, the thermal fumes maintain a stratified layer. The thermal fumes do not disperse in the dimensionless tunnel height range from z^* = 0 to 0.5. The evacuation environment under this condition is maintained in a tunnel fire.

Figure 7 shows the contour map of the temperature rise in the tunnel under the condition of the average dimensionless quasi-steady heat release rate Q^*_m = 0.0775. Froude number Fr is in the range of 0.245 to 0.345 as a variable parameter. The thermal fumes disperse widely in the case of a small Froude number. The thermal fumes maintain stratified layers in the sections downstream and upstream from the fire source in the range of Fr = 0.245 to 0.321. On the other hand, the thermal fumes cannot maintain a stratified layer in the downstream section when the Froude number Fr is 0.345. The thermal fumes diffuse on the road surface of the tunnel in the downstream section.

Figure 8 shows the temperature rise distribution in the height direction in the sections downstream and upstream from the fire source under the condition of the average dimensionless quasi-steady heat release rate Q^*_m = 0.111. Froude number Fr is in the range of 0.299 to 0.375 as a variable parameter. The rapid rise in temperature is from z^* = 0.5 or 0.6 on the upstream side and the thermal fumes form a stratified layer. Downstream, the rise in temperature gradually increases from z^* = 0.3 or 0.4. The maximum temperature rise occurs close to the ceiling. The state of stratification is ambiguous.

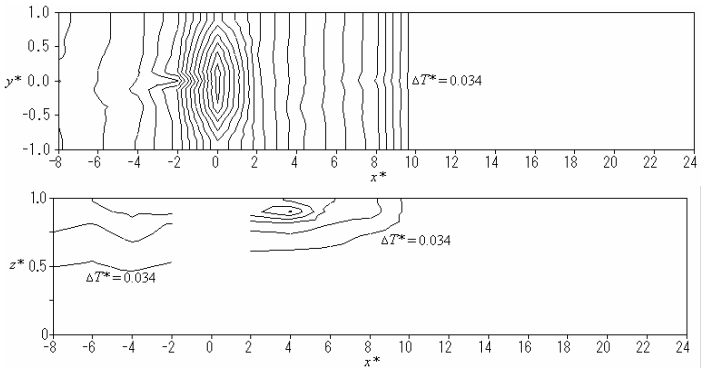

(a) $Q^*_m = 0.0316$, $Fr = 0.25$

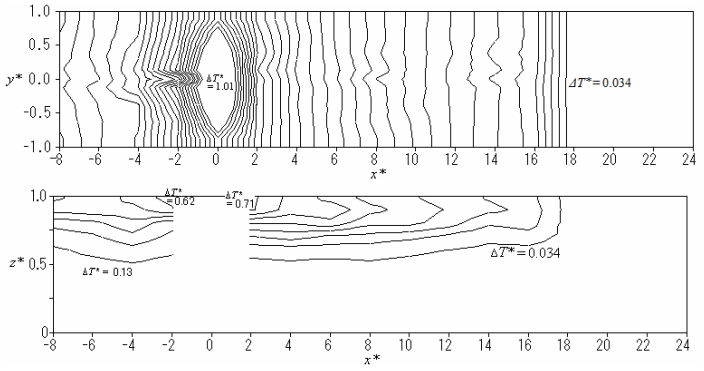

(b) $Q^*_m = 0.0775$, $Fr = 0.26$

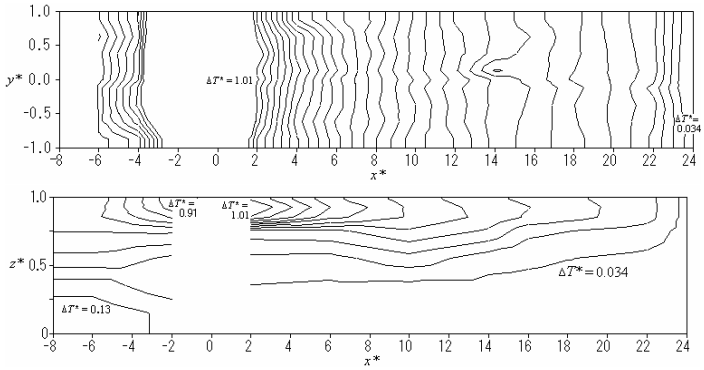

(c) $Q^*_m = 0.182$, $Fr = 0.27$

Fig. 6 Contour maps of the temperature rise at the ceiling and longitudinal section of the tunnel for three different heat release rates in the case of Froude number Fr nearly constant at 0.26. The temperature at the ceiling and longitudinal section is divided into 30 and 10 levels, respectively

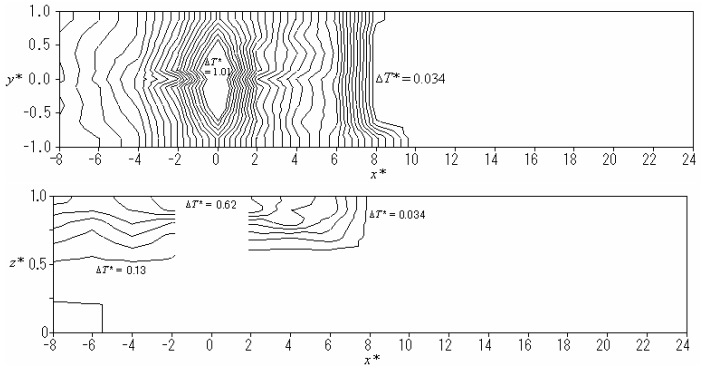

(a) $Fr = 0.345$

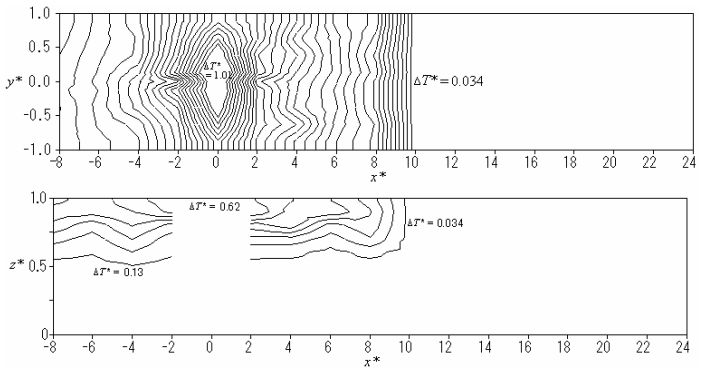

(b) $Fr = 0.321$

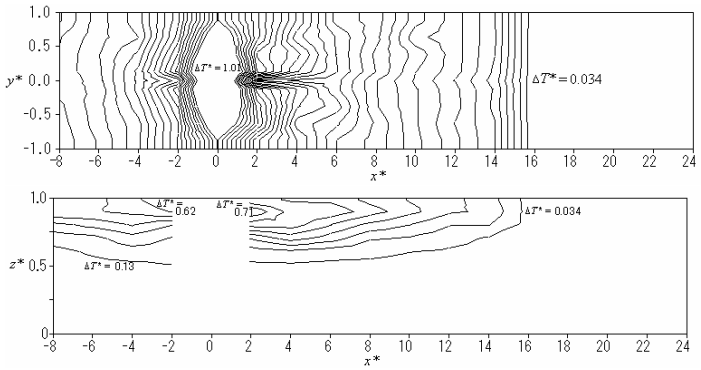

(c) $Fr = 0.280$

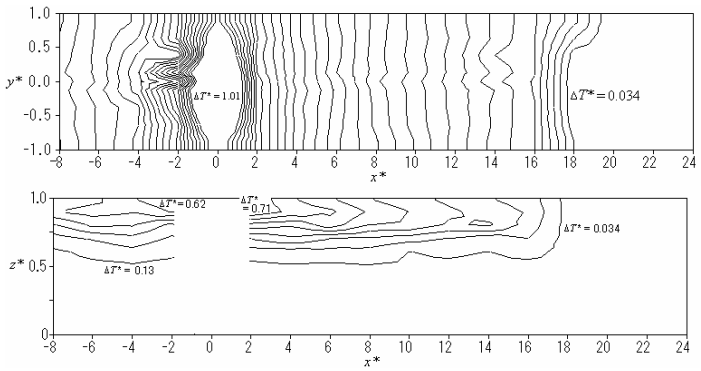

(d) $Fr = 0.245$

Fig. 7 Contour maps for four different Froude numbers in the case of the average dimensionless quasi-steady heat release rate Q^*_m at 0.0775. The temperature at the ceiling and longitudinal section is divided into 30 and 10 levels, respectively. When the ambient temperature T_0 is 298 K, the dimensionless temperature $T^* = 0.034$ and 1.01 corresponds to the temperature rise $\delta T = 10$ and 300 K, respectively.

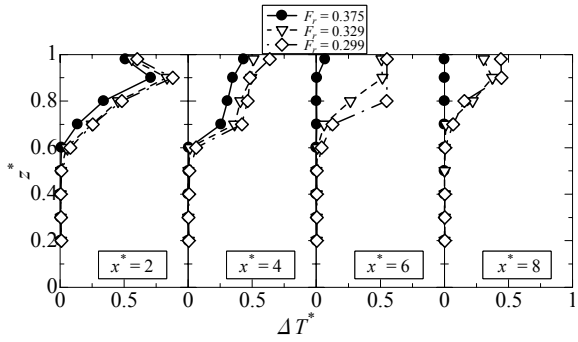

(a) Temperature distribution upstream from the fire source (positions: x^* = 2, 4, 6, and 8)

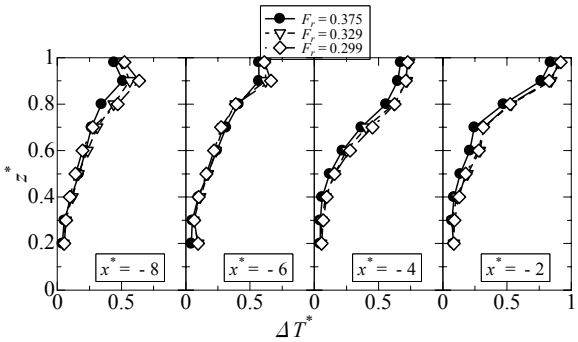

(b) Temperature distribution downstream from the fire source (positions: x^* = −2, −4, −6, and −8)

Fig. 8 Rise in temperature distribution in the direction of the height in four different positions in the case of Q^*_m = 0.111

6. Thermal fume height

It is important to have a clear understanding of the height of the boundary between the thermal fumes maintaining a stratified layer and the fresh air flowing under the thermal fumes, in order to secure safe evacuation in a tunnel fire. An in-depth discussion of this topic is presented in this section. The height of the thermal fume layer was defined based on the temperature distribution in the direction of the height. The height of the thermal fume layer is the position at which the rise in temperature is 10 K (T^* = 0.034) higher than the ambient temperature. For example, in the case of the thermal fumes distributed in a tunnel as shown in Fig. 9, a group of three points (A, B, and C) upstream and a group of three points (a, b, and c) downstream from the fire source were used for temperature distribution. The average height at the three points of each group (A, B, and C or a, b, and c) was defined as the thermal fume height. The thermal fume height at the thermal fume tip of position D was excluded from the arithmetic average.

Figure 10 shows the relationship between the dimensionless average thermal fume height H^*_{dT} and the ratio of the dimensionless heat release rate Q^* to the Froude number Fr. Figures 10(a) and 10(b) show the thermal fume height at the upstream and downstream side, respectively. Over this experimental data range, the thermal fume height upstream from the fire source decreased linearly with the increase of the parameter Q^*/Fr. A relational expression was determined by using the least squares method as follows:

$$H^*_{DT} = -0.183\frac{Q^*}{Fr} + 0.651 \quad (1)$$

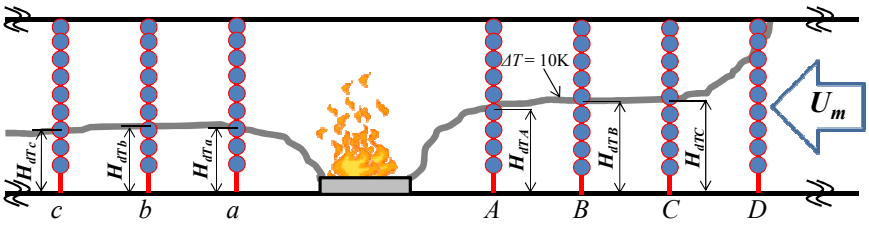

Fig. 9 Definition of the height of the thermal fumes: H_{dT} shows the smoke layer height defined by the temperature rise (δT = 10 K). Position D at the thermal fume tip was excluded from the definition of the height of the thermal fumes

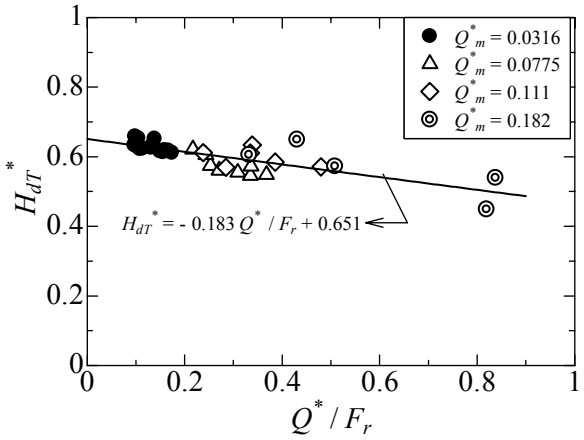

(a) Upstream from the fire source

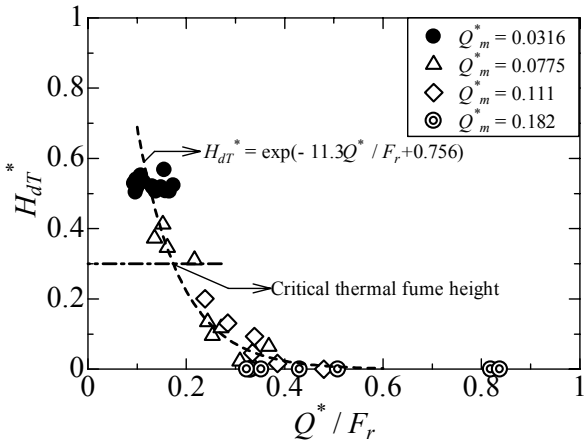

(b) Downstream from the fire source

Fig. 10 Modeling of the thermal fume height as a function of Q^*/Fr (δT = 10 K)

The dimensionless thermal fume height is H^*_{dT} = 0.5 determined by Expression (1) in the case of Q^*/Fr = 0.9. There were no thermal fumes in the lower half of the tunnel in this situation. Furthermore, Expression (1) gave 15 MW as the heat release rate of the fire in the case of a full-scale tunnel (5-m height, 10-m width, 2-m/s emergency ventilation velocity). Expression (1) indicated that the evacuation environment under thermal fumes was sufficiently secured when the heat release rate of a full-scale fire was not greater than 15 MW. In the case of the thermal fume height downstream from the fire source in Fig. 10(b), the thermal fume height decreased exponentially with the increase of the

parameter Q^*/Fr. When the value of parameter Q^*/Fr was 0.4 or greater, thermal fumes were diffused to the road surface. A relational expression was determined by using the least squares method as follows:

$$H^*_{DT} = \exp\left(-11.3\frac{Q^*}{Fr} + 0.756\right) \quad (2)$$

The critical height of thermal fumes was assumed to be 1.5 m, the height of a human's eyes, as the safety criterion for the evacuation environment in a tunnel fire of a full-scale tunnel. In this case, dimensionless thermal fume height H^*_{dT} and parameter Q^*/Fr were 0.3 and 0.173, respectively. Therefore, Expression (2) indicated that the evacuation environment downstream from the full-scale fire was safe, under the conditions where the heat release rate of the fire in the full-scale tunnel (5-m height, 10-m width, 2-m/s ventilation velocity) was 6 MW or less.

7. Conclusions

Tunnel fire experiments were conducted using a large-scale model tunnel with completely turbulent flow and considering the heat transfer characteristics of the tunnel wall. The temperature at many positions, velocity of longitudinal ventilation, and the heat release rate of the fire source were measured, and used to investigate the temperature distribution of the backlayering thermal fumes. The following results were obtained in the range of Q^*/Fr = 0.1 to 0.8 as the governing scaling parameter, and in the range of Q^*_m = 0.0316 to 0.182 as the heat release rate :

1. The rapid rise in temperature is from z^* = 0.5 or 0.6 on the upstream side and the thermal fumes form a stratified layer.
2. The rise in temperature gradually increases from z^* = 0.3 or 0.4 downstream from the fire source. The maximum value of the rise in temperature is at a point close to the ceiling. The state of stratification is ambiguous.
3. The thermal fume height upstream from the fire source decreases linearly with the increase of the parameter Q^*/Fr by Expression (1).
4. The thermal fume height downstream from the fire source decreases exponentially with the increase of the parameter Q^*/Fr by Expression (2). When the value of parameter Q^*/Fr was 0.4 or greater, thermal fumes were diffused to the road surface.

References

(1) Fire and Disaster Management Agency, 2006 version, White Paper on Fire Defense (in Japanese), (2006).
(2) PIARC Committee on Road Tunnels Operation (C3.3), Systems and Equipment for Fire and Smoke Control in Road Tunnels, (2007).
(3) Thomas, P.H., The Movement of Smoke in Horizontal Passage Against an Air Flow, Fire Research Note No. 723 (1968), Fire Research Station.
(4) Danziger, N.H. and Kennedy, W.D., Longitudinal Ventilation Analysis for the Glenwood Canyon Tunnels, *Proceedings of the 4th International Symposium on Aerodynamics and Ventilation of Vehicle Tunnels* (1982), pp. 169-186.
(5) Oka, Y. and Atkinson, G.T., Control of Smoke Flow in Tunnel Fires, *Fire Safety Journal*, Vol. 25 (1995), pp. 305-322.
(6) Mizutani, T., Horiuchi, K., et al., Report on tunnel fire test – the tunnel fire test for longitudinal ventilation, Technical Note of Public Works Research Institute, No. 1876,

(1982).
(7) Wu, Y. and Baker, M.Z.A., Control of Smoke Flow in Tunnel Fires using Longitudinal Ventilation Systems – A Study of the Critical Velocity, *Fire Safety Journal*, Vol. 35 (2000), pp. 363-390.
(8) Lee, S.R. and Ryou, S.H., An Experimental Study of the Effect of the Aspect Ratio on the Critical Velocity in Longitudinal Ventilation Tunnel Fires, *Journal of Fire Sciences*, Vol. 23 (2005), pp. 119-138.
(9) Lannermark, A. and Ingason, H., Fire Spread and Flame Length in Large-Scale Tunnel Fires, *Fire Technology*, Vol. 42 (2006), pp. 283-302.
(10) Roh, J.S., Yang, S.S., Ryou, H.S., Yoon, M.O. and Jeong, Y.T., An Experimental Study on the Effect of Ventilation Velocity on Burning Rate in Tunnel Fires – Heptane Pool Case, *Building and Environment*, Vol. 43 (2008), pp. 1225-1231.
(11) Yamada, T., Watanabe, Y., Matsushima, S., Oka, Y., Kurioka, H., Kuwana, H. and Satoh, H., Ventilation Criteria for Preventing Backing Layer of Smoke in Case of Tunnel Fire, Report of National Research Institute of Fire and Disaster, No. 83 (1997), pp. 37-46.
(12) Wang, Q., Kawabata, N. and Ishikawa, T., Evaluation of Critical Velocity Employed to Prevent the Backlayering of Thermal Fume during Tunnel Fires, *Proceedings of the International Conference on ACFD*, (2000), pp. 404-411.
(13) Vantelon, J.P., Guelzim, A., Quach, D. and Son, D.K., Investigation of Fire-Induced Smoke Movement in Tunnels and Stations: An Application to the Paris Metro, *Proceedings of the Third International Symposium on Fire Safety Science*, (1991), pp. 907-918.
(14) Saito, N., Sekizawa, A., Yamada, T., Yanai, E., Watanabe, Y. and Miyazaki, S., Study Report on Fire Performance in Special Space of Use of Underground Space, Fire Defence Research Datum No. 29 (1994).
(15) Lee, S.R. and Ryou, H.S., A Numerical Study on Smoke Movement in Longitudinal Ventilation Tunnel Fires for Different Aspect Ratio, *Building and Environment*, Vol. 41 (2006), pp. 719-725.
(16) Kunikane, Y., Kawabata, N., Yamada, T. and Shimoda, A., Influence of Stationary Vehicles on Backlayering Characteristics of Fire Plume in a Large Cross Section Tunnel, *JSME International Journal*, *Series B*, Vol. 49, No. 3 (2006), pp. 594-600.
(17) Kikumoto, T., Kawabata, N., Maruyama, D. and Yamada, M., Model Tests on Fire Smoke Behavior in a Small Road Tunnel for Passenger Cars, *Journals of the Japan Society of Civil Engineers*, *Division F*, Vol. 63, No. 3 (2007), pp. 361-373.
(18) Kunikane, Y., Kawabata, N., Takekuni, K., Ishikawa, T. and Shimoda, A., Heat Release Rate of Gasoline Poll Fire in Large Cross Sectional Tunnel, *Transactions of the Japan Society of Mechanical Engineers*, *Series B*, Vol. 69, No. 685 (2003), pp. 2044-2051.